

1N-20
198106
24P

**NASA
Technical
Memorandum**

NASA TM - 108433

**PERFORMANCE ASSESSMENT OF LOW PRESSURE
NUCLEAR THERMAL PROPULSION**

By H.P. Gerrish Jr. and G.E. Doughty

Propulsion Laboratory
Science and Engineering Directorate

December 1993

(NASA-TM-108433) PERFORMANCE
ASSESSMENT OF LOW PRESSURE NUCLEAR
THERMAL PROPULSION (NASA) 24 p

N94-21860

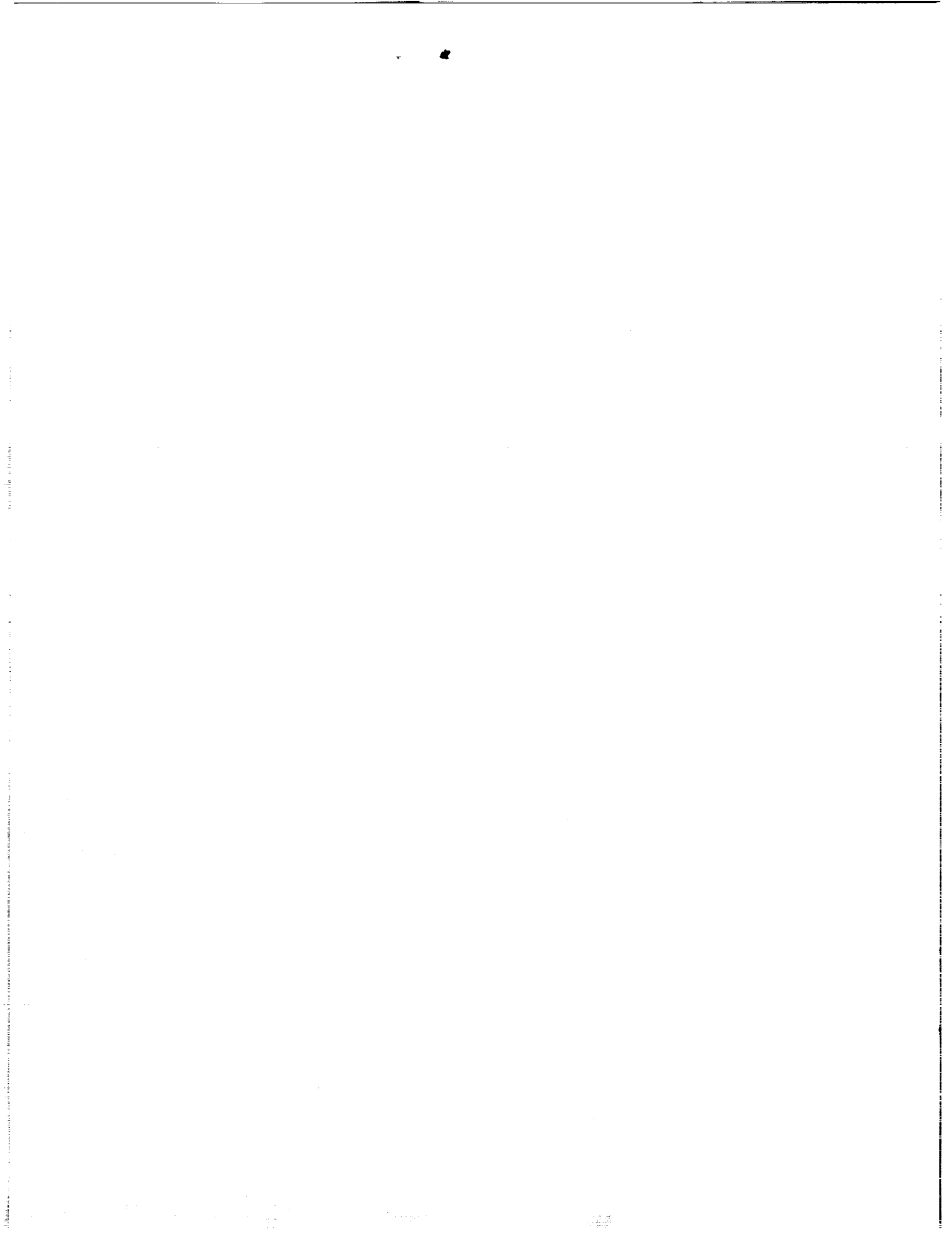
Unclas

G3/20 0198106



National Aeronautics and
Space Administration

George C. Marshall Space Flight Center



REPORT DOCUMENTATION PAGE

Form Approved
OMB No. 0704-0188

Public reporting burden for this collection of information is estimated to average 1 hour per response, including the time for reviewing instructions, searching existing data sources, gathering and maintaining the data needed, and completing and reviewing the collection of information. Send comments regarding this burden estimate or any other aspect of this collection of information, including suggestions for reducing this burden, to Washington Headquarters Services, Directorate for Information Operations and Reports, 1215 Jefferson Davis Highway, Suite 1204, Arlington, VA 22202-4302, and to the Office of Management and Budget, Paperwork Reduction Project (0704-0188), Washington, DC 20503.

1. AGENCY USE ONLY (Leave blank)	2. REPORT DATE December 1993	3. REPORT TYPE AND DATES COVERED Technical Memorandum
----------------------------------	---------------------------------	--

4. TITLE AND SUBTITLE Performance Assessment of Low Pressure Nuclear Thermal Propulsion	5. FUNDING NUMBERS
--	--------------------

6. AUTHOR(S) H.P. Gerrish, Jr. and G.E. Doughty	
--	--

7. PERFORMING ORGANIZATION NAME(S) AND ADDRESS(ES) George C. Marshall Space Flight Center Marshall Space Flight Center, Alabama 35812	8. PERFORMING ORGANIZATION REPORT NUMBER
---	--

9. SPONSORING / MONITORING AGENCY NAME(S) AND ADDRESS(ES) National Aeronautics and Space Administration Washington, DC 20546	10. SPONSORING / MONITORING AGENCY REPORT NUMBER NASA TM - 108433
--	--

11. SUPPLEMENTARY NOTES Prepared by Propulsion Laboratory, Science and Engineering Directorate.
--

12a. DISTRIBUTION / AVAILABILITY STATEMENT Unclassified—Unlimited	12b. DISTRIBUTION CODE
--	------------------------

13. ABSTRACT (Maximum 200 words) A low pressure nuclear thermal propulsion (LPNTP) system, which takes advantage of hydrogen dissociation/recombination, has been proposed as a means of increasing engine specific impulse (Isp). This paper examines the effect of hydrogen dissociation/recombination on LPNTP Isp. A two-dimensional computer model was used to show that the optimum chamber pressure is approximately 100 psia (at a chamber temperature of 3,000 K), with an Isp ~15 s higher than at 1,000 psia. At high chamber temperatures and low chamber pressures, the increase in Isp is due to both lower average molecular weights caused by dissociation and added kinetic energy from monatomic hydrogen recombination. Monatomic hydrogen recombination increases the Isp more than hydrogen dissociation. Variations in the mole fraction of monatomic hydrogen are similar to variations in static pressure along the axial nozzle position. Most recombination occurs close to the nozzle throat. Practical variations in nozzle geometry have minimal impact on recombination. Other models, which can simulate a wider range of nozzle designs, should be used in the future. The uncertainty of the hydrogen kinetic reaction rates at high temperatures (~3,000 K) affects the accuracy of the analysis and should be verified with simple bench tests.

14. SUBJECT TERMS low pressure nuclear thermal propulsion, hydrogen dissociation/recombination, specific impulse, reaction rate coefficient	15. NUMBER OF PAGES 25
	16. PRICE CODE NTIS

17. SECURITY CLASSIFICATION OF REPORT Unclassified	18. SECURITY CLASSIFICATION OF THIS PAGE Unclassified	19. SECURITY CLASSIFICATION OF ABSTRACT Unclassified	20. LIMITATION OF ABSTRACT Unlimited
---	--	---	---

TABLE OF CONTENTS

	Page
INTRODUCTION	1
HYDROGEN DISSOCIATION/RECOMBINATION SENSITIVITIES.....	2
KINETICS MODEL.....	3
RESULTS	4
Pressure Sensitivity.....	4
Temperature Sensitivity	6
Nozzle Contour Sensitivity	7
Kinetics Sensitivity.....	11
Best Potential LPNTP Design	14
CONCLUSIONS	14
RECOMMENDATIONS.....	15
REFERENCES.....	16

PRECEDING PAGE BLANK NOT FILMED

LIST OF ILLUSTRATIONS

Figure	Title	Page
1.	Mole fraction of hydrogen dissociated to monatomic hydrogen.....	1
2.	Baseline LPNTP nozzle design.....	3
3.	Isp versus P_o ($T_o = 3,000$ K).....	5
4.	Isp versus P_o ($T_o = 3,000$ K).....	5
5.	X_H versus axial nozzle position.....	5
6.	One-dimensional Isp increase from hydrogen dissociation and recombination versus chamber pressure.....	6
7.	Isp versus P_o ($T_o = 3,200$ K).....	6
8.	Isp versus P_o ($T_o = 3,200$ K).....	7
9.	Wall throat radius of curvature.....	9
10.	X_H and P versus X ($P_o = 10$ psia).....	9
11.	X_H and T versus X ($P_o = 10$ psia).....	10
12.	X_H and P versus X ($P_o = 100$ psia).....	10
13.	X_H and T versus X ($P_o = 100$ psia).....	10
14.	Isp dependence on kinetic reaction rate magnitude	13
15.	Isp dependence on the Arrhenius temperature exponent for H.....	13
16.	Isp dependence on the Arrhenius temperature exponent for H_2	13

LIST OF TABLES

Table	Title	Page
1.	Kinetic reaction rate coefficient equations.....	4
2.	Effects of nozzle geometry variations on recombination.....	8
3.	Effects of various k_H and k_{H_2} equations on ODK Isp.....	11
4.	Isp variations with reaction rate accuracy ($T_o = 3,000$ K).....	12
5.	Isp variations with reaction rate accuracy ($T_o = 3,200$ K).....	12

DEFINITION OF SYMBOLS AND ABBREVIATIONS

Symbol	Definition
atm	atmosphere
A	pre-exponential coefficient
B	activation energy
Isp	specific impulse
k	reaction rate coefficient
k_H	reaction rate coefficient for monatomic hydrogen
k_{H_2}	reaction rate coefficient for molecular hydrogen
K	degrees Kelvin
N	temperature dependence of the pre-exponential factor
P	static pressure
P_0	stagnation chamber pressure
psia	pounds per square inch absolute
r^*	throat radius
R	degrees Rankine
T	static temperature
T_0	stagnation chamber temperature
X	axial nozzle position from the throat
X_H	mole fraction of monatomic hydrogen

NONSTANDARD ABBREVIATIONS

C&W	Cohen & Westberg
LPNTP	low pressure nuclear thermal propulsion
ODE	one-dimensional equilibrium
ODF	one-dimensional frozen
ODK	one-dimensional kinetics
RWTD	normalized wall radius of curvature downstream of nozzle throat
RWTU	normalized wall radius of curvature upstream of nozzle throat
TDK	two-dimensional kinetics



TECHNICAL MEMORANDUM

PERFORMANCE ASSESSMENT OF LOW PRESSURE NUCLEAR THERMAL PROPULSION

INTRODUCTION

An increase in Isp for nuclear thermal propulsion systems is desirable for reducing the propellant requirements and cost of future applications, such as the Mars transfer vehicle. Several previous design studies have suggested that the Isp could be increased substantially with hydrogen dissociation/recombination. Hydrogen molecules (H_2), at high temperatures and low pressures, will dissociate to monatomic hydrogen (H) (fig. 1). The reverse process (i.e., formation of H_2 from H) is exothermic. The exothermic energy increases the kinetic energy and, therefore, increases the Isp.

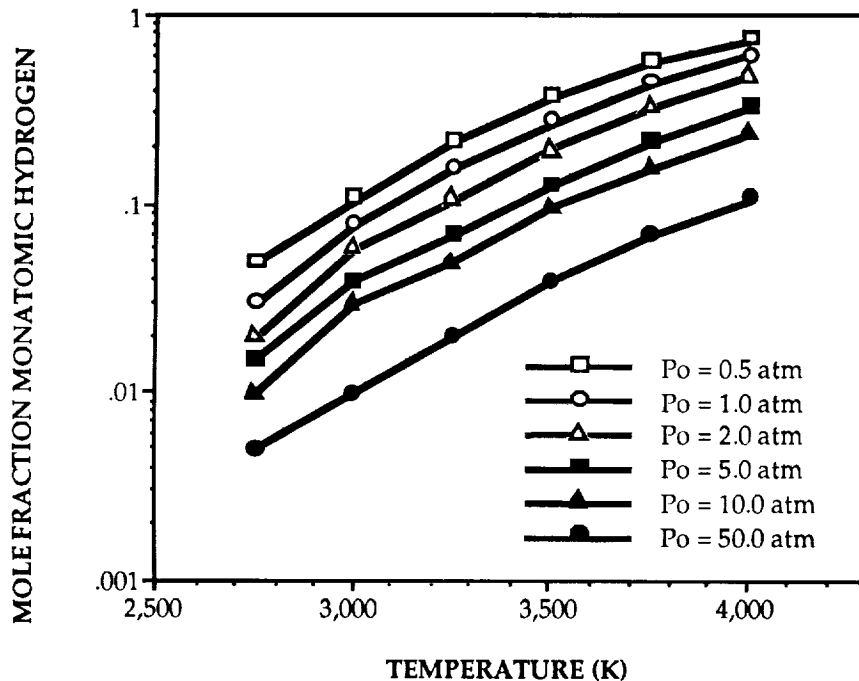


Figure 1. Mole fraction of hydrogen dissociated to monatomic hydrogen.¹

The LPNTP system is expected to maximize the hydrogen dissociation/recombination and Isp by operating at high chamber temperatures and low chamber pressures. The process involves hydrogen flow through a high-temperature, low-pressure fission reactor and out a nozzle. The high temperature (~3,000 K) of the hydrogen in the reactor is limited by the temperature limits of the reactor material. The chamber pressure is about 1 atm because lower pressures decrease the engines thrust-to-weight ratio below acceptable limits. This study assumes that hydrogen leaves the reactor and enters the nozzle at the 3,000 K equilibrium dissociation level. The computer model used begins with equilibrium at the nozzle inlet.

Hydrogen dissociation in the reactor does not affect LPNTP performance like dissociation in traditional chemical propulsion systems, because energy from the reactor resupplies energy lost due to hydrogen dissociation. Recombination takes place in the nozzle due primarily to a drop in temperature as the Mach number increases. However, as the Mach number increases beyond the nozzle throat, the static pressure and density of the flow decreases which minimizes the recombination. The ideal LPNTP Isp at 3,000 K and 10 psia is 1,160 s due to the added energy from fast recombination rates. The actual Isp depends on the finite kinetic reaction rates which affect the amount of monatomic hydrogen recombination before the flow exits the nozzle.

An LPNTP system has other technical issues (e.g., flow instability and two-phase flow) besides hydrogen dissociation/recombination which affect the systems practicality. In this study, only the effects of hydrogen dissociation/recombination are examined.

HYDROGEN DISSOCIATION/RECOMBINATION SENSITIVITIES

A computer code was configured to model an LPNTP engine. The baseline nozzle design is shown in figure 2. The following model parameters were chosen based on a conventional conical nozzle design to keep the calculations simple for an initial study:

- 5.2336-in throat radius
- 27.6:1 nozzle contraction ratio
- 200:1 nozzle expansion ratio
- Conical diverging nozzle section
- Hydrogen propellant
- 10 psia chamber pressure
- 3,000 K chamber temperature
- Nominal reaction rate coefficient

Equations from Cohen & Westberg(C&W)²

$$k_H = 3.2 \cdot 10^{15}$$

$$k_{H_2} = (1.0 \cdot 10^{17}) \cdot T^{-0.6}$$

- All nozzle flow in one zone
- Neglect boundary layer calculations and heat loss.

Unless otherwise stated, all parameters are maintained at the baseline value for each computer run.

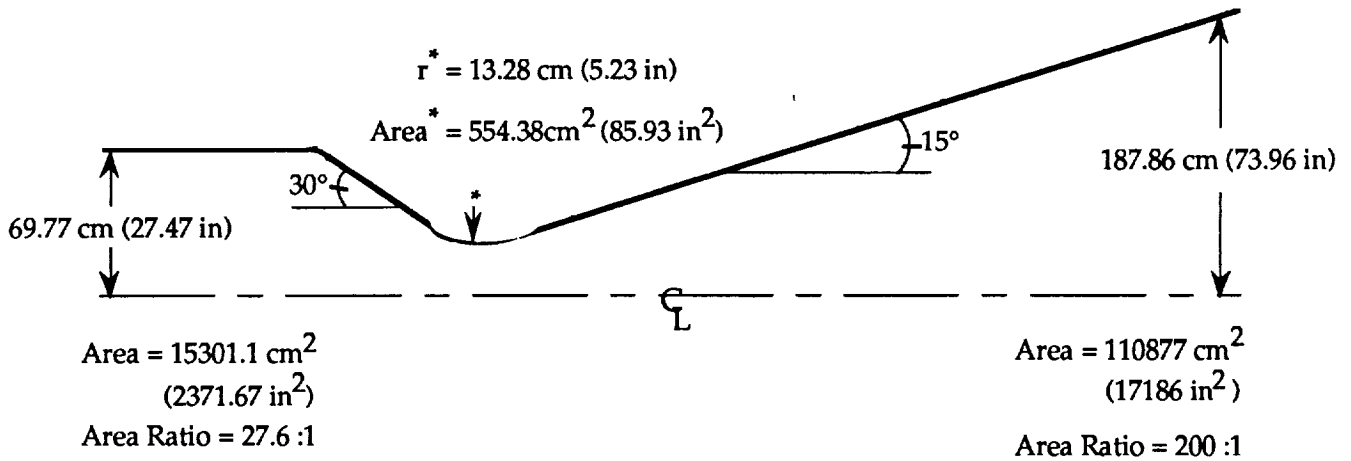


Figure 2. Baseline LPNTP nozzle design.

KINETICS MODEL

The two-dimensional kinetics (TDK) nozzle performance computer program³ was used to determine the effect of various parameters on hydrogen dissociation/recombination and Isp. TDK simulates an inviscid flow from the start of nozzle contraction to the nozzle exit. The one-dimensional equilibrium (ODE) option of TDK was used to calculate the upper Isp limit due to shifting molar species concentrations in the expansion process. The one-dimensional frozen (ODF) option of TDK was used to calculate the lower Isp limit due to frozen molar species concentrations in the expansion process. The one-dimensional kinetics (ODK) option of TDK accounts for the effects of finite chemical kinetics. Both ODE and ODK calculations provide data in the axial direction only, and the properties for each cross section are constant. The TDK option calculates changes in the radial direction and uses two third-body reactions for hydrogen (H_2 , H):

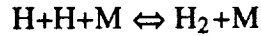


The reaction rate coefficient equations (k_{H_2} and k_H) for each of the above reactions are in the Arrhenius form, which is written as:

$$K = AT^{-N} e^{\frac{-1,000B}{RT}} \quad (3)$$

Empirical data from C&W was used to determine the constants in the Arrhenius equation for both hydrogen third-body reactions. There is an uncertainty in k_H and k_{H_2} , which affects the accuracy of the computed Isp. The uncertainty is due to the substantial variation in the results of hydrogen reaction rate experiments. Table 1 shows the forward kinetic k_H and k_{H_2} equations obtained from C&W, from the national aerospace plane (NASP) rate constant committee of the NASP high-speed propulsion technology team,⁴ and from the default equations used in the TDK. The C&W equations were used in this study.

Table 1. Kinetic reaction rate coefficient equations.



<u>Standard TDK³</u>		
M = Ar	$k = 6.4 \cdot 10^{17} T^{(-1)}$	
M = H	$k = 25 \cdot k(\text{Ar})$	
M = H ₂	$k = 4 \cdot k(\text{Ar})$	
<u>Cohen and Westberg²</u>		
M = H	$k = 1 \cdot 10^{15}$	Low
	$k = 3.2 \cdot 10^{15}$	Nominal
	$k = 1.0 \cdot 10^{16}$	High
M = H ₂	$k = 5 \cdot 10^{16} \cdot T^{(-0.6)}$	Low
	$k = 1.0 \cdot 10^{17} \cdot T^{(-0.6)}$	Nominal
	$k = 2.0 \cdot 10^{17} \cdot T^{(-0.6)}$	High
<u>NASP Equations⁴</u>		
M = H	$k = 1.5 \cdot 10^{19} \cdot T^{(-1.0)}$	
M = H ₂	$k = 1.8 \cdot 10^{18} \cdot T^{(-1.0)}$	

Units = cm⁶/(Mole²·s)

RESULTS

Pressure Sensitivity

This section shows the effects of chamber pressure (P_o) on the Isp. The ODK and TDK Isp curves are close to equilibrium (ODE) at high P_o , but approach frozen flow (ODF) at low P_o (fig. 3). As P_o decreases from 1,000 to 100 psia, both ODK Isp and TDK Isp increase. At 100 psia, figure 4 shows the ODK Isp to be approximately 1,007 s, which is 27 s greater than the ODF Isp. From 100 psia down to 10 psia, the ODK Isp and TDK Isp change is minimal. Below 10 psia, the ODK Isp increases like frozen flow due to a lower average molecular weight caused by greater dissociation and less recombination. Because P_o below 1 atm was considered impractical, 10 psia is the lower limit of P_o . At 10 psia, the ODK Isp is 1,005 s, but is only 14 s greater than the ODF Isp.

The mole fraction of monatomic hydrogen (X_H) entering the nozzle is 17.3 percent with P_o at 10 psia and 5.9 percent with P_o at 100 psia (fig. 5). The X_H decreases in the nozzle due to monatomic hydrogen recombination. Inside the nozzle, there is 3-percent recombination at 100 psia and 1.25-percent recombination at 10 psia, as shown in figure 5. Greater recombination from higher pressures is the reason why the difference between ODK Isp and ODF Isp is greater at 100 psia than at 10 psia, as shown in figure 4.

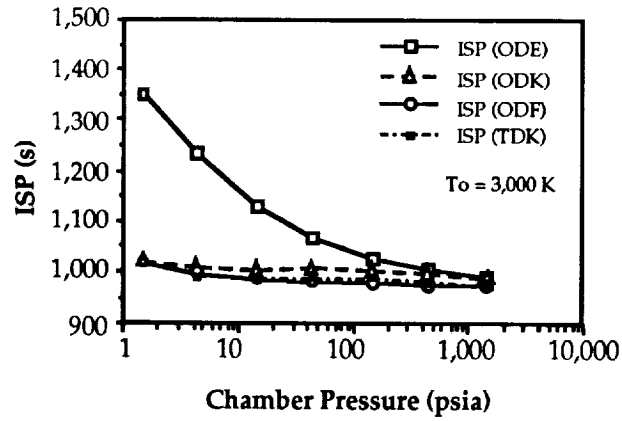


Figure 3. Isp versus P_o ($T_o = 3,000$ K).

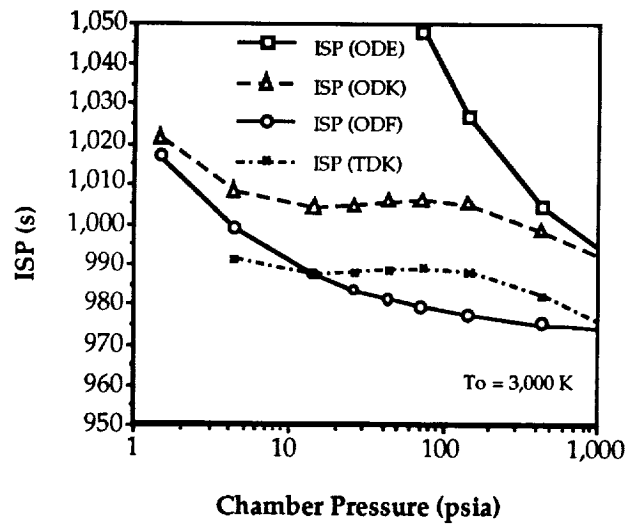


Figure 4. Isp versus P_o ($T_o = 3,000$ K).

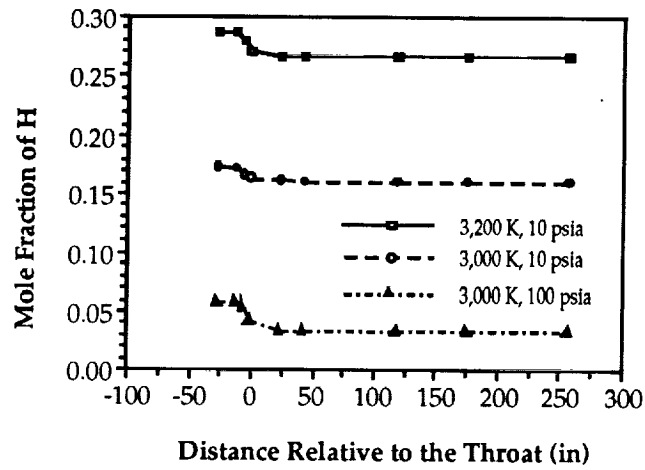


Figure 5. X_H versus axial nozzle position.

The amount of one-dimensional Isp increase above frozen flow Isp (at 1,000 psia and 3,000 K) due to hydrogen dissociation (lower molecular weights) and monatomic hydrogen recombination (added kinetic energy) is shown in figure 6, at various pressures.

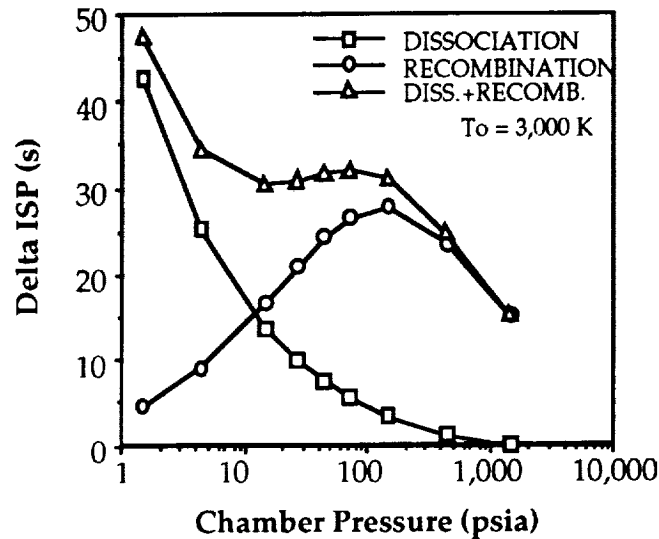


Figure 6. One-dimensional Isp increase from hydrogen dissociation and recombination versus chamber pressure.

Temperature Sensitivity

This section shows the effect on Isp by increasing the chamber temperature (T_o) to 3,200 K. Plots illustrating Isp versus P_o at 3,200 K are shown in figures 7 and 8. The Isp is almost constant from 10 to 100 psia. At 100 psia, the ODK Isp is 1,066 s, which is 45 s greater than the ODF Isp. Thus, increasing T_o from 3,000 K to 3,200 K will increase the ODK Isp by approximately 60 s.

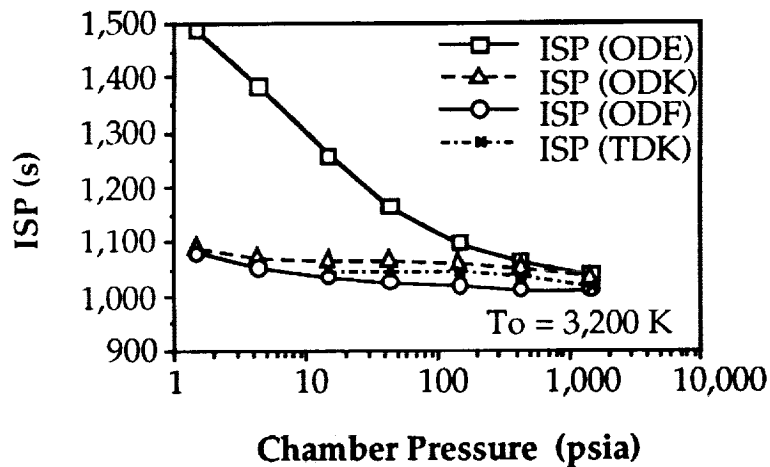


Figure 7. Isp versus P_o ($T_o = 3,200$ K).

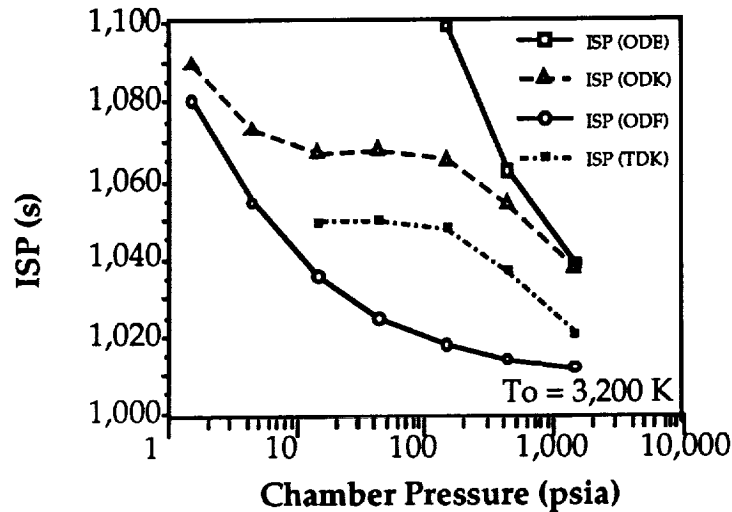


Figure 8. Isp versus P_o ($T_o = 3,200$ K).

The effect of chamber temperature on the X_H is shown in figure 5. Increasing T_o from 3,000 K to 3,200 K, at 10 psia, increases X_H at the nozzle inlet to 28.6 percent. Results show 2-percent recombination inside the nozzle. In addition, the exiting X_H at 10 psia is higher at 3,200 K than at 3,000 K. Greater X_H , greater recombination, and higher T_o will all increase the Isp due to smaller average molecular weights and greater kinetic energy in the nozzle exhaust flow.

Nozzle Contour Sensitivity

The ODK results show X_H at the nozzle exit to be 16.17 percent for the baseline nozzle contour. This section shows the sensitivity of the nozzle contour (within TDK limits) on monatomic hydrogen recombination.

Table 2 displays the effects of nozzle geometry variations on X_H . Results show that by varying either the contraction ratio or the expansion ratio, there is no effect on the recombination. Holding the area ratios constant and lowering the nozzle converging angle from 30° to 10° , lowers the X_H at the nozzle exit to 15.9 percent, but increases the TDK Isp by only 3 s over the baseline. Lowering the nozzle diverging angle from 15° to 5° lowers the X_H at the nozzle exit to 15.7 percent, and increases the TDK Isp 19 s above the baseline value. The higher Isp for small diverging cone angles is due to a greater axial component of exhaust velocity created by less divergence of the nozzle flow at the exit. Small converging and diverging cone angles require longer nozzles which may be impractical. For example, decreasing the diverging angle from 15° to 5° increases the total nozzle length from 300 in to over 800 in.

Variation of the nozzle throat geometries is also considered because figure 5 indicates that most recombination occurs around the nozzle throat. Larger throat radii increase the recombination and TDK Isp (table 2). By increasing the throat radius from 5.23 to 10.0 in, the X_H at the nozzle exit decreases to 15.6 percent, and the TDK Isp increases 6 s greater than the baseline TDK Isp. However, increasing the throat radius from 5.23 to 10 in almost doubles the nozzle length, and increases

the thrust and mass flow rate by 365 percent. Other results show that the increased nozzle length increases propellant stay time in the nozzle, and indicate minimum changes in pressure and temperature at the nozzle throat compared with baseline LPNTP. Thus, some additional recombination could be caused by a longer stay time around the nozzle throat.

The normalized wall radius of curvature downstream of the throat (RWTD), and the normalized wall radius of curvature upstream of the throat (RWTU) are displayed in figure 9.

Table 2. Effects of nozzle geometry variations on recombination.

Parameters	Percent Mole Fraction of H at Various Nozzle Area Ratios					Isp (s)	
	Inlet (ODE)	1.5 (ODE)	Throat (ODK)	1.5 (ODK)	Exit (ODK)	ODK	TDK
Contraction Ratio low = 10 nominal = 27.6 high = 50	17.30 17.30 17.30	N/A	16.42 16.41 16.42	N/A	16.17 16.17 16.17	N/A	988 988 988
Expansion Ratio low = 75 nominal = 200 high = 500	17.30 17.30 17.30	N/A	16.41 16.41 16.41	N/A	16.17 16.17 16.17	N/A	976 988 995
Converging Angle low = 10° nominal = 30° high = 50°	17.30 17.30 17.30	N/A	16.17 16.41 16.44	N/A	15.93 16.17 16.30	N/A	991 988 988
Diverging Angle low = 5° nominal = 15° high = 45°	17.30 17.30 17.30	N/A	16.42 16.41 16.41	N/A	15.74 16.17 16.30	1,009 1,005	1,007 988 844
R* (inches) low = 2.0 nominal = 5.23 high = 10.0	17.30 17.30 17.30	N/A	16.81 16.41 16.05	N/A	16.71 16.17 15.62	N/A	982 988 994
RWTU low = 0.5 nominal = 1.5 high = 3.0	N/A	16.64 16.64 16.64	16.56 16.41 16.22	16.33 16.25 16.01	N/A	1,004 1,005 1,007	N/A
RWTD low = 0.5 nominal = 0.4 high = 1.5	N/A	16.64 16.64 16.64	16.43 16.41 16.40	16.28 16.25 16.18	N/A	1,004 1,005 1,005	N/A
Contour Cone Bell (100% length)	N/A	16.64 16.64	16.41 16.41	16.25 16.29	16.17 16.24	1,005 1,004	988 993

Note: All cases were run at $P_o = 10$ psia and $T_o = 3,000$ K.

By doubling the RWTU, the X_H at the 1.5 area ratio in the diverging section decreases from 16.25 to 16.01 percent, and the ODK Isp increases from 1,005 to 1007 s. In addition, by increasing RWTD from 0.4 to 1.5, X_H at the 1.5 area ratio in the diverging section of the nozzle decreases from 16.25 to 16.18 percent, but the ODK Isp is almost constant. The effect due to changes in RWTU are greater than changes in RWTD because a larger RWTU increases both the converging nozzle length and the propellant stay time in the part of the nozzle which has higher pressures and flow densities.

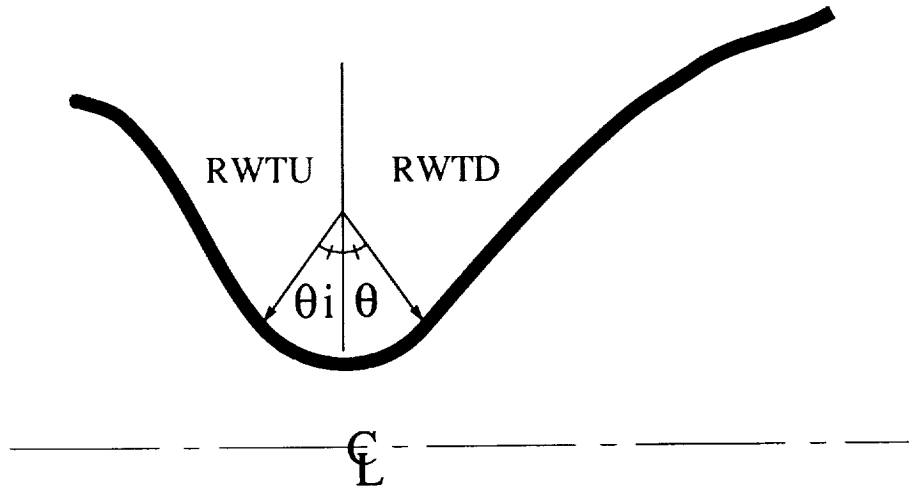


Figure 9. Wall throat radius of curvature.

The one-dimensional variations of pressure, temperature, and X_H throughout the LPNTP nozzle are displayed in figures 10 and 11. Both figures show most recombination occurring around the throat. The change in X_H throughout the nozzle is very similar to changes in pressure. At the point where recombination stops, the pressure is close to 0 psia. However, the temperature continues to drop with no changes in X_H . These results indicate that low static temperatures allow recombination to begin, but low static pressures and flow densities limit the amount of recombination.

The one-dimensional variations of pressure, temperature, and X_H throughout the baseline nozzle at 100-psia chamber pressure are shown in figures 12 and 13. As before, the recombination stops when the static pressure is close to 0 psia. There is greater recombination at higher pressures even though X_H at the nozzle inlet is less. Thus, recombination appears greater in nozzle regions with high static pressures. The longer the stay time in these regions, the greater the amount of recombination.

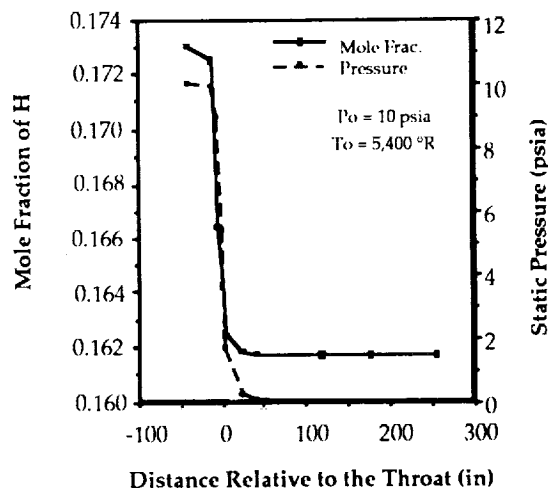


Figure 10. X_H and P versus X ($P_0 = 10$ psia).

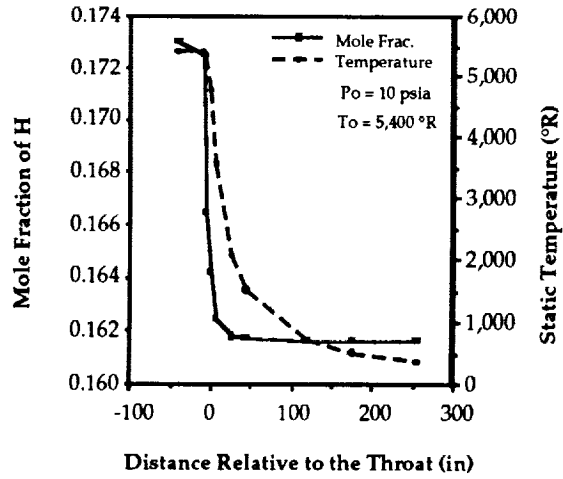


Figure 11. X_H and T versus X ($P_o = 10$ psia).

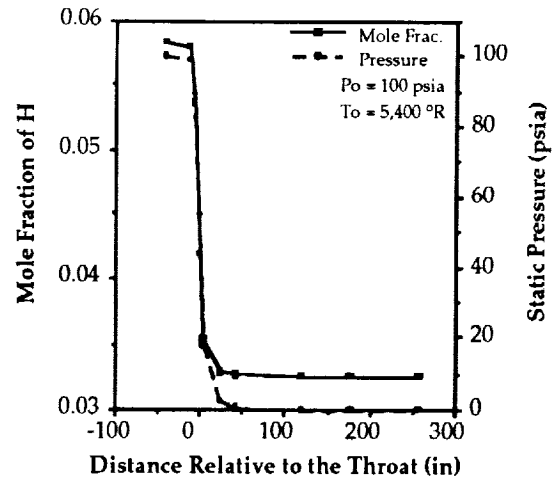


Figure 12. X_H and P versus X ($P_o = 100$ psia).

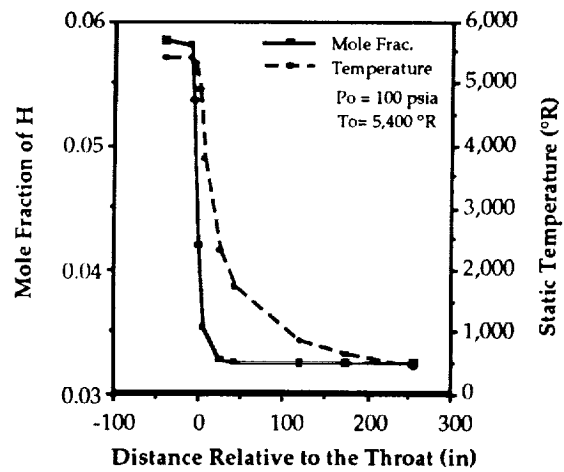


Figure 13. X_H and T versus X ($P_o = 100$ psia).

The effect of a bell nozzle's diverging contour on recombination was also examined. Table 2 shows the effects of a bell nozzle contour on the X_H and Isp. The bell nozzle has a slightly larger X_H at the nozzle exit, and an ODK Isp 1 s lower than the baseline conical nozzle. These results could be due to the bell nozzle having a greater diverging angle beyond the throat, which reduces the stay time in pressure regions needed for recombination. The bell nozzle has a greater TDK Isp because of less divergence losses at the nozzle exit.

Kinetics Sensitivity

The effects of hydrogen kinetic reaction rate uncertainty and key parameters in the Arrhenius equation were also analyzed. Although differences in reaction rate coefficients should not affect the results of a comparative study such as this, it will be an important aspect in ensuring TDK accuracy and Isp predictions. Previously shown in table 1 were three different sets of k_H and k_{H_2} equations. The effect of each equation on ODK Isp is shown in table 3.

Table 3. Effects of various k_H and k_{H_2} equations on ODK Isp.

<u>Hydrogen Reaction Rate Coefficient Equations</u>	<u>ODK Isp (s)</u>	
	<u>$T_o = 3,000\text{ K}$</u>	<u>$T_o = 3,200\text{ K}$</u>
C&W	1,005	1,068
NASP	1,006	1,073
Default TDK	1,008	1,076

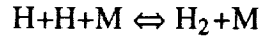
Results show a small difference in ODK Isp between the three sets of k_H and k_{H_2} equations. Each set of equations was determined from experimental reaction rates. The uncertainty for each set of k_H and k_{H_2} equations is due to either scatter in experimental data or experiment type.

Table 1 shows the C&W k_H and k_{H_2} equations used to determine the impact of uncertainty on Isp. The nominal equations were recommended by C&W. The high and low equations of k_H and k_{H_2} at 3,000 K represent the fastest and slowest rate limits, respectively, based on the C&W level of uncertainty. The effects on Isp caused by C&W uncertainty are shown in table 4. There is an Isp increase when either/or both k_H and k_{H_2} become larger. Note, there is a slightly greater effect on Isp when varying k_H instead of k_{H_2} due to the greater uncertainty of the monatomic equation. The ODK Isp goes from 999 s with the slowest rates to 1,014 s with the fastest rates. Table 5 shows similar results, but with T_o equal to 3,200 K. At 3,200 K, the ODK Isp goes from 1,056 s with the slowest rates to 1,085 s with the fastest rates. Higher temperatures decrease the Isp accuracy because of greater uncertainty. The maximum variation in Isp due to uncertainty is significant and should not be ignored.

The A and N parameters in the Arrhenius equation were examined to determine the impact on the Isp. By multiplying the nominal value of A in k_H and k_{H_2} by various assumed multipliers, the ODK Isp will increase as shown in figure 14. Rates which are 10 times faster than nominal will increase the ODK Isp by approximately 30 s. The TDK Isp is more sensitive to variations of N in the

Arrhenius equation for k_{H_2} than k_H , as shown in figures 15 and 16. Decreasing N for k_{H_2} from 1.0 to 0.2, increases the TDK Isp by about 44 s. Isp effects when varying both A and N for each computer run were not examined.

Table 4. Isp variations with reaction rate accuracy ($T_o = 3,000$ K).



M = H ₂	M = H		
	Low	Nominal	High
Low	999* (982)**	1,002 (985)	1,009 (992)
Nominal	1,001 (985)	1,005 (988)	1,011 (994)
High	1,007 (990)	1,009 (993)	1,014 (997)

Isp (ODE) = 1,159 s

Isp (ODF) = 991 s

$T_o = 3,000$ K

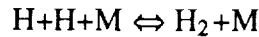
$P_o = 10$ psia

$A_e/A^* = 200$

*ODK Isp (s)

**TDK Isp (s)

Table 5. Isp variations with reaction rate accuracy ($T_o = 3,200$ K).



M = H ₂	M = H		
	Low	Nominal	High
Low	1,056* (1,039)**	1,064 (1,047)	1,079 (1,062)
Nominal	1,061 (1,043)	1,068 (1,050)	1,081 (1,064)
High	1,068 (1,051)	1,074 (1,056)	1,085 (1,067)

Isp (ODE) = 1,297 s

Isp (ODF) = 1,041 s

$T_o = 3,200$ K

$P_o = 10$ psia

$A_e/A^* = 200$

*ODK Isp (s)

**TDK Isp (s)

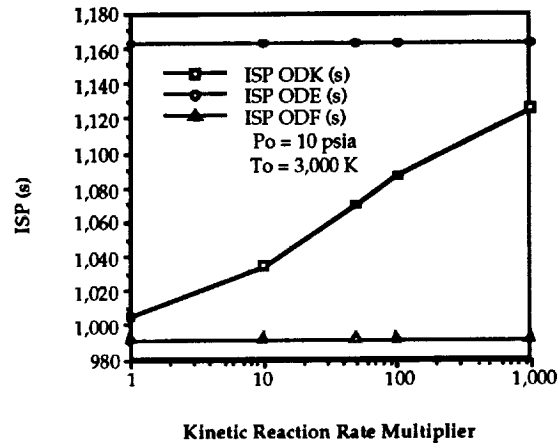


Figure 14. Isp dependence on kinetic reaction rate magnitude.

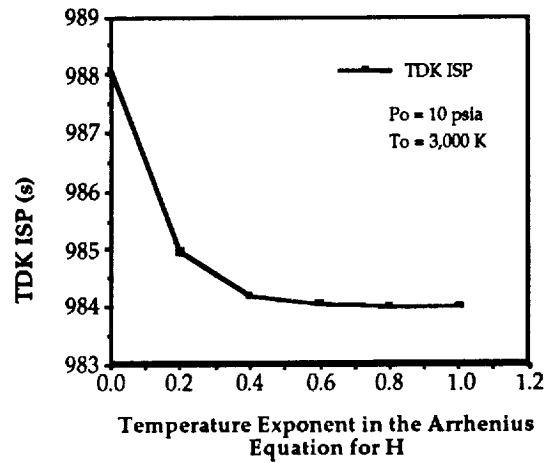


Figure 15. Isp dependence on the Arrhenius temperature exponent for H.

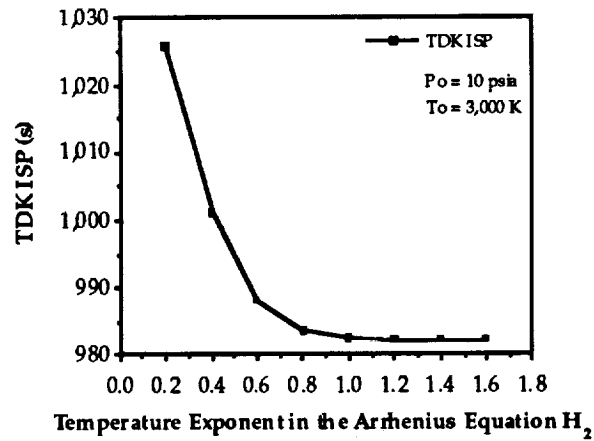


Figure 16. Isp dependence on the Arrhenius temperature exponent for H₂.

Best Potential LPNTP Design

Based on the parameters examined, the optimum value for each parameter and the fastest reaction rates from C&W were input into the TDK model. The following input parameters are different from the baseline:

- Converging angle = 5°
- Contraction ratio = 7.41:1
- RWTU = 3.0
- RWTD = 1.5
- Bell nozzle with diverging section
78-percent baseline diverging nozzle length
- $P_o = 44$ psia
- $T_o = 3,200$ K
- $k_H = 1.0 \cdot 10^{16}$
- $k_{H_2} = (2.0 \cdot 10^{17}) \cdot T^{-0.6}$.

The total nozzle length is the same as the baseline nozzle length. The ODK Isp result is 1,080 s. In addition, the ODK thrust is 6,845 lbf and the mass flow rate is 6.338 lbm/s. The ODK Isp result is slightly less than the largest ODK Isp from table 5, which uses the fastest rates with baseline nozzle geometry. This result shows minimum impact on ODK Isp from optimum nozzle geometry.

CONCLUSIONS

TDK Isp is close to equilibrium flow at high P_o and close to frozen flow at low P_o . With T_o at 3,000 K, the maximum TDK Isp and maximum difference between ODK Isp and ODF Isp occurs at $P_o \sim 100$ psia, due to increased monatomic hydrogen recombination. The Isp is ~ 15 s higher at a P_o of 100 psia than at 1,000 psia. The optimum P_o indicates a greater impact on Isp from recombination than from lower average molecular weights. A P_o of 3,200 K increases both the dissociation (decrease in the average hydrogen molecular weight) and the recombination of the flow. These characteristics boost the Isp above the value that would be obtained by only considering temperature effects.

Examination of various nozzle geometries showed a minimum impact on recombination and Isp. The significant changes that did occur were related to a more efficient use of two-dimensional nozzle flow. Most recombination occurs around the nozzle throat due to low static temperatures which foster recombination. Low static pressures and flow densities limit the amount of recombination downstream of the throat.

Finally, the uncertainty of the k_H and k_{H_2} , at high T_o , has a significant impact on the Isp predictions. There is a large difference between ODE and ODF Isp's at a lower P_o , and the ODK Isp could be anywhere between, depending on the assumed reaction rate. The slow k_H and k_{H_2} used in this study cause the ODK Isp to approach the ODF Isp at low static pressures.

RECOMMENDATIONS

Since the LPNTP Isp predictions were closer to frozen flow Isp than ideal equilibrium Isp at low P_o , more extensive calculations, using a TDK model that accounts for boundary layer effects, and nonadiabatic flow are not recommended at this time.

Faster kinetic reaction rates will increase both the monatomic hydrogen recombination and the Isp. Because there is an uncertainty with the high temperature values of k_H and k_{H_2} , accurate hydrogen dissociation/recombination bench tests are recommended to determine if the actual reaction rates are different than the published reaction rates used in this study. High temperature subscaled nozzle tests with load cells and flowmeters are recommended to determine actual Isp, because actual nozzle flow characteristics (e.g., boundary layer effects) might affect the amount of hydrogen dissociation/recombination.

Based on the results of this study, the chamber pressure recommended is 190 psia for a 3,000 K chamber temperature. This chamber pressure is above hydrogen's critical pressure (188 psia) to minimize two-phase flow problems in the feed system (e.g., flow oscillations). Operating at 190 psia has an Isp slightly less than at 100 psia, but produces a higher thrust than at 10 psia and has a higher Isp than at 1,000 psia. In addition, the nozzle should have a bell diverging section to shorten the nozzle length and minimize divergence losses. The nozzle's converging/throat section should be designed to maximize the recombination.

Finally, TDK only uses conical converging nozzle sections. Other kinetic computer models which can vary the converging nozzle contour should be investigated to determine the effects on Isp.

REFERENCES


1. Benton, D.: "CREST" computer program, version 4, 1988.
2. Cohen, N., and Westberg, K.: "Chemical Kinetic Data Sheets for High Temperature Chemical Reactions." *J Phys Chem. Ref Data*, vol. 12, No. 3, 1983, pp. 531–590.
3. Nickerson, G.R., Coats, D.E., Dang, A.L., Dunn, S.S., and Kehtarnavaz, H.: "Two-Dimensional Kinetics (TDK) Nozzle Performance Computer Program." Software and Engineering Associated, Inc., NAS8-36863, March 1989.
4. Oldenberg, R.: "Hypersonic Combustion Kinetics—Status Report of the Rate Constant Committee, NASP High-Speed Propulsion Technology Team." NASP Tech Memo 1107, May 1990.

APPROVAL

**PERFORMANCE ASSESSMENT OF LOW PRESSURE NUCLEAR THERMAL
PROPULSION**


By H.P. Gerrish Jr. and G.E. Doughty

The information in this report has been reviewed for technical content. Review of any information concerning Department of Defense or nuclear energy activities or programs has been made by the MSFC Security Classification Officer. This report, in its entirety, has been determined to be unclassified.



J.P. MCCARTY
Director, Propulsion Laboratory

☆ U.S. GOVERNMENT PRINTING OFFICE 1993-533-108/00001


PRECEDING PAGE BLANK NOT FILMED



